Crystal structure of a humanized Fab fragment of anti-tissue-factor antibody in complex with tissue factor

Umeharu Ohto,[a] Ryuta Mizutani,[a] Mitsuaki Nakamura,[b] Hideki Adachi[b] and Yoshinori Satow[a*]

[a]Graduate School of Pharmaceutical Sciences, University of Tokyo, 7-3-1 Hongo, Bunkyo, Tokyo 113-0033, Japan, and [b]Fuji Gotemba Research Labs, Chugai Pharmaceutical Co., Ltd., 1-135 Komakado, Gotemba, Shizuoka 412-8513, Japan. E-mail: satow@mol.f.u-tokyo.ac.jp

Tissue factor (TF) is a membrane-anchored protein that initiates the extrinsic cascade of blood coagulation. TF forms a complex with serine protease Factor VIIa, and then activates Factor X zymogen to Factor Xa, leading to the blood coagulation. Humanized anti-TF antibody hATR-5 strongly inhibits TF-initiated blood coagulation, and is of potential use for various thrombotic diseases. The Fab fragment of antibody hATR-5 is obtained for crystallization. The crystal structure of the complex of the Fab with extracellular domains of human TF was determined with the molecular replacement method, and refined to an *R* factor of 0.196 at 2.1 Å resolution. All the complementarity-determining regions (CDRs) of the Fab are involved in interaction with the C-terminal-side extracellular domain of TF through 19 hydrogen bonds. The interface between the Fab and TF molecules contains 15 water molecules, and yields buried surface areas as wide as 2000 Å^2. The TF surface in the interface is possibly involved in the activation of Factor X, by forming a transient ternary complex of Factor X-TF-Factor VIIa. Electrostatic interactions are predominantly observed between the heavy-chain CDRs and TF. These hydrogen-bonding and electrostatic interactions together with the wide buried areas contribute to the high affinity of the antibody toward TF, leading to the effective inhibition of the TF-initiated blood coagulation.

Keywords: blood coagulation; humanized antibody; Fab fragment; tissue factor; crystal structure.

1. Introduction

Tissue factor (TF), a cell surface glycoprotein receptor, interacts with the serine protease Factor VIIa and its macromolecular substrate Factor X, and triggers the extrinsic blood coagulation cascade. In case of the vessel injuries, TF exposed to circulating blood forms the TF-Factor VIIa complex which activates Factor X to Xa (Butenas *et al*., 2002; Rapaport *et al*., 1995). These processes subsequently result in the fibrin deposition and platelet activation. In addition to the normal hemostasis, TF is involved in various pathogenic states relating to the diseases that involve blood coagulation such as atherosclerosis and thrombosis (Wilcox *et al*., 1989; Wakefield *et al*., 1997).

Antibodies are widely used for various therapeutic purposes utilizing their high specificities and affinities toward antigens (Berger *et al*., 2002; Mountain *et al*., 1992). Humanized anti-TF antibody hATR-5 strongly inhibits the TF activity *in vivo*, and therefore is of potential use for some thrombosis diseases (Adachi *et al*., 2001). The crystal structure of the Fab fragment of hATR-5 in complex with extracellular domains of TF is expected to clarify structural basis for recognition of TF by the antibody and also for effective inhibition of the TF-mediated blood coagulation. Structural comparison with the other anti-TF antibodies D3H44 and 5G9 (Faelber *et al*., 2001; Huang *et al*., 1998) is carried out so as to provide clear insights for the high affinity of hATR-5 toward the TF epitope.

2. Materials and methods

2.1. Sample preparation

Humanized anti-tissue factor antibody hATR-5 comprising of the frameworks of the human immunoglobulin 4 (κ) antibody and the grafted CDR (complementarity-determining region) residues from a mouse monoclonal anti-TF antibody was prepared by Chugai Pharmaceutical Co. Ltd. (Adachi *et al*., 2001). The hATR-5 Fab was prepared with papain digestion, with an enzyme-to-substrate molar ratio of 1:20 in a solution of 18 mM cysteine, 1.8 mM EDTA, 84 mM NaCl, 44 mM NaH_2PO_4 of pH 7.0. The Fab was purified as reported (Yokoyama *et al*., 2000). The extracellular region (residues 1 to 210) of human TF was expressed in the *E. coli* JM109 strain following the reported procedure (Waxman *et al*., 1992). The complex of the hATR-5 Fab with TF is prepared by mixing the Fab and TF in a molar ratio of 1:1.2. Excess TF was removed using the Superdex200 gel-filtration column (Amersham Biosciences) equilibrated with 50 mM Na acetate pH 5.0. The purified Fab-TF complex is concentrated to 20 mg/ml.

2.2. Crystallization

Crystallization attempts were carried out with the hanging-drop vapor-diffusion method at 277 K using 50 mM HEPES-Na buffer pH 7.5 containing 5 % 2-propanol, and 10 % PEG 4000 as a reservoir. Crystals with sizes of 0.30×0.20×0.15 mm^3 were obtained with macroseeding within 3-4 weeks. Using a rotating-anode generator, these crystals diffracted X-rays up to 3.0 Å resolution. They belong to the space group $P2_12_12$ with cell parameters of a = 103 Å, b = 266 Å, and c = 42.3 Å. The asymmetric unit contains one Fab-TF complex, showing a high Matthews coefficient (Matthews, 1968) of 4.0 Å^3/Da and a solvent content of 70 %.

2.3. Data collection and structure determination

X-ray diffraction data at 2.1 Å resolution were collected on beamline BL38B1 of SPring-8, Hyogo, Japan, with a Quantum-4R CCD detector. Diffraction frames were processed with program MOSFILM and subsequently reduced into intensities with SCALA and POSTREF of the CCP4 suit (CCP4, 1994). The data collection is summarized in Table 1. The structure of the Fab-TF complex was determined with the molecular replacement method using program CNS (Brünger *et al*., 1998). The crystal structures of the extracellular domains of human tissue factor (PDB accession code 2HFT) and of the D3H44 Fab (1JPT) were used as search models. After the rotation and translation searches, the model obtained by rigid-body refinements at 4.0 Å resolution gave an *R* factor of 0.363. This model was then subjected to several cycles of the simulated-annealing refinements followed by manual model fitting with TURBO-FRODO (Roussel & Cambillau, 1995) through gradual incorporation of higher resolution data. Refinement statistics are also summarized in Table 1. Buried surface areas of the molecules were calculated with CNS using a probe radius of 1.4 Å. Structural geometries were analyzed with PROCHECK (Laskowski *et al*., 1993). The amino-acid numbering and CDR definition of antibody are made in accordance with the standard notation (Kabat *et al*., 1991). The coordinates of the complex have been deposited with the Protein Data Bank (accession code 1UJ3).

 © 2004 International Union of Crystallography • Printed in Great Britain – all rights reserved

Table 1

Statistics on diffraction data collection and structure refinement [a]

Resolution range (Å)	37.1 - 2.1
Wavelength (Å)	1.0000
Temperature (K)	100
Number of crystals used	2
Number of observed reflections	306,177 (23,527)
Number of unique reflections	64,872 (8,041)
R_{merge} (I) [b]	0.087 (0.183)
Completeness	0.94 (0.81)
R [c] / R_{free} [d]	0.196 / 0.227
Number of non-hydrogen atoms	
Protein	4,913
Water	476
Main-chain torsion angles (%) in	
Most favored regions	88.0
Additionally allowed regions	10.8
Generously allowed regions	0.7
Disallowed regions	0.5
Rms deviations from idealities	
Bond length (Å)	0.010
Bond angle (deg.)	1.65

[a] The parenthesized values are for the highest resolution shell between 2.2 Å and 2.1 Å.
[b] $R_{merge}(I) = \Sigma|I - \langle I \rangle|/\Sigma I$, where I is observed diffraction intensity.
[c] $R = \Sigma||F_o| - |F_c||/\Sigma|F_o|$, where F_o and F_c are observed and calculated structure amplitudes, respectively.
[d] R_{free} is an R value for a 10 % subset of all the reflections, which was not used in the crystallographic refinement.

3. Results and discussion

3.1. Overall structure of the hATR-5 Fab complexed with TF

The Overall structure of the complex as determined at 2.1 Å resolution is shown in Figure 1. The data collection and refinement statistics listed in Table 1 give an estimated coordinate error of 0.22 Å (Luzzati, 1952). All residues are within the allowed regions of the Φ-Ψ plot, with the exception of Ala 51L whose conformation is commonly observed in the most L2 CDR loops (Mizutani *et al*., 1995). The N-terminal domain 1 (residues 1 to 107) of TF is located in lower electron densities than the rest of the TF molecule, and the first five residues are omitted from the modeled structure. Molecular contacts involved with the domain 1 is only observed for Tyr 51 that is located near the crystallographic two-fold axis. Clear electron-densities are observed for the C-terminal domain 2 (residues 108 to 210) which is in interaction with the Fab. This domain is subdivided into two β-sheets, one consisting of three strands A (residues 112-119), B (122-130), and E (174-177), and the other of four strands C (152-158), C' (166-170), F (185-193) and G (199-210).

3.2. Interaction between the hATR-5 Fab and TF molecules

The TF residues in the interaction with the Fab consist of Lys 122 in the B strand and of 19 residues from the four-stranded β-sheet, as shown in Figure 2. The CDRs of L1, L2, and L3 of the Fab form five hydrogen bonds with TF, and the CDRs H1, H2, and H3 form 14 hydrogen bonds as summarized in Table 2. Among the TF residues located in the interface, Lys 169, Arg 200, and Lys 201 show electrostatic complementarity to the negatively-charged residues of the heavy-chain CDRs. The N^{ζ} atom of Lys 169 in the C' strand forms a salt bridge to the $O^{\beta 1}$ atom of Asp 95H which is placed at the bottom of a pocket formed by the L3 and H3 loops. The Lys 169 N^{β} atom is also hydrogen-bonded to the Gly 97H O atom. The Arg 200 side-chain is hydrogen-bonded to the Asp 31H O atom, to the Ser 96H O, and to a water molecule bound to the Asp 95H O. The Lys 201 N^{β} atom forms a salt bridge to the Asp 52aH $O^{\beta 1}$ atom and two hydrogen-bonds to the Lys 30H and Tyr 32H main-chain O atoms in the H1 loop. The heavy-chain CDRs of the hATR-5 Fab shows larger contribution toward recognition of TF than the light-chain CDRs, as is pointed out for antigen recognition seen in antibodies in complex with protein antigens (Davies *et al*., 1990).

The L3 residues of Gly 92L, Glu 93L, and Ser 94L are in a β-strand conformation and form an anti-parallel β-sheet with the C' strand of TF. The distance between the Gly 92L O and Lys 169 N atoms is 2.8 Å, and that of the Ser 94L N and Thr 167 O is 2.9 Å. Therefore the L3 conformation which is classified to the canonical type-1 structure (Chothia *et al*., 1989) plays an important role in the recognition of the β-strand structure of TF. A total of 15 water molecules are accommodated in the Fab-TF interface.

The buried surface areas upon the complex formation are as wide as 2025 Å^2, and are considerably wider than those observed for the other Fab-TF complexes; the values for the D3H44 and 5G9 complexes are 1850 Å^2 (Faelber *et al*., 2001) and 1814 Å^2 (Huang *et al*., 1998), respectively. Figure 3 shows the electrostatic potential surfaces of the interface regions of the hATR-5 Fab and TF molecules. The negatively-charged surface of the Fab interface is well suited for electrostatic complementarity to the positively-charged surface of TF.

The binding site for Factor X is proposed to consists of residues Tyr 157, Lys 159, Ser 163, Gly 164, Lys 166, and Tyr 185 (Kirchhofer *et al*., 2000; Venkateswarlu *et al*., 2002), and is located in the vicinity of the C' strand. Therefore the hATR-5 binding to these epitopes blocks the TF surface from Factor X, and prevents the initiation of the blood coagulation cascade.

Table 2

Hydrogen bonds between the hATR-5 and TF molecules

CDR	Fab atom		TF atom		Distance (Å)
L1	Gln 27L	$O^{\varepsilon 1}$	Lys 122	N^{ζ}	3.0
L2	Tyr 50L	O^{η}	Asn 171	$N^{\delta 2}$	2.8
L3	Gly 92L	O	Lys 169	N	2.8
	Ser 94L	N	Thr 167	O	2.9
	Ser 94L	O^{γ}	Thr 167	N	2.9
H1	Lys 30H	O	Lys 201	N	2.8
	Asp 31H	O	Arg 200	$N^{\eta 1}$	2.6
	Tyr 32H	O	Lys 201	N^{ζ}	2.8
	Tyr 33H	O^{η}	Thr 154	$O^{\gamma 1}$	2.8
	Tyr 33H	O^{η}	Gln 190	$O^{\varepsilon 1}$	2.6
H2	Asp 52aH	$O^{\delta 2}$	Tyr 156	O^{ζ}	2.6
	Asp 52aH	$O^{\delta 2}$	Gln 190	$O^{\varepsilon 1}$	2.9
	Asp 52aH	$O^{\delta 1}$	Lys 201	N^{ζ}	2.7
	Asn 55H	$N^{\delta 2}$	Asp 204	$O^{\delta 2}$	2.7
H3	Asp 95H	$O^{\delta 1}$	Lys 169	N^{ζ}	2.8
	Ser 96H	O	Arg 200	$N^{\eta 2}$	2.8
	Gly 97H	O	Lys 169	N^{ζ}	3.0
	Tyr 98H	O^{η}	Lys 149	O	2.6
	Tyr 98H	O^{η}	Asn 171	$N^{\delta 2}$	3.2

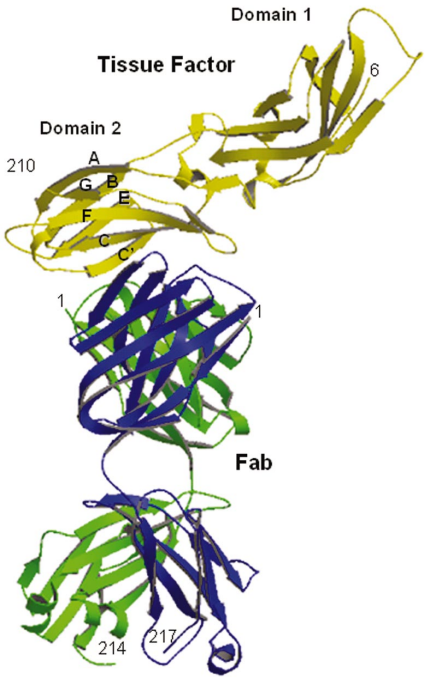

Figure 1

Ribbon representation of the hATR-5 Fab in complex with human TF. The Fab light-chain is drawn in green, the heavy-chain in blue, and TF in yellow. The first and last residues of the polypeptide chains are added with their numbers, and the β-strands of the TF domain 2 are labeled sequentially as A to G. The Fab recognizes mainly the β-sheet consisting of four strands C, C', F, and G of TF. This figure was prepared with program MOLSCRIPT (Kraulis, 1991).

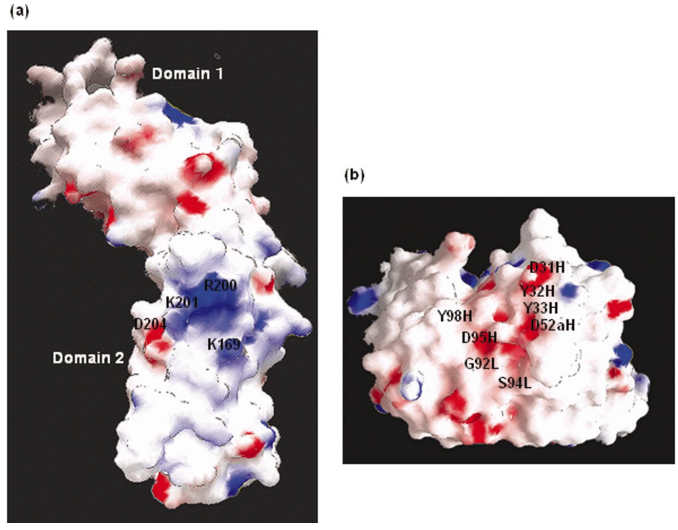

Figure 3

Electrostatic representations of the Fab and TF surfaces. (a) Fab. (b) TF. Charged side-chains in the interface between the Fab and TF molecules are indicated with labels for their residues. Positive and negative potentials are shown in blue and red, respectively. The figures were prepared using program GRASP (Nicholls *et al*., 1991).

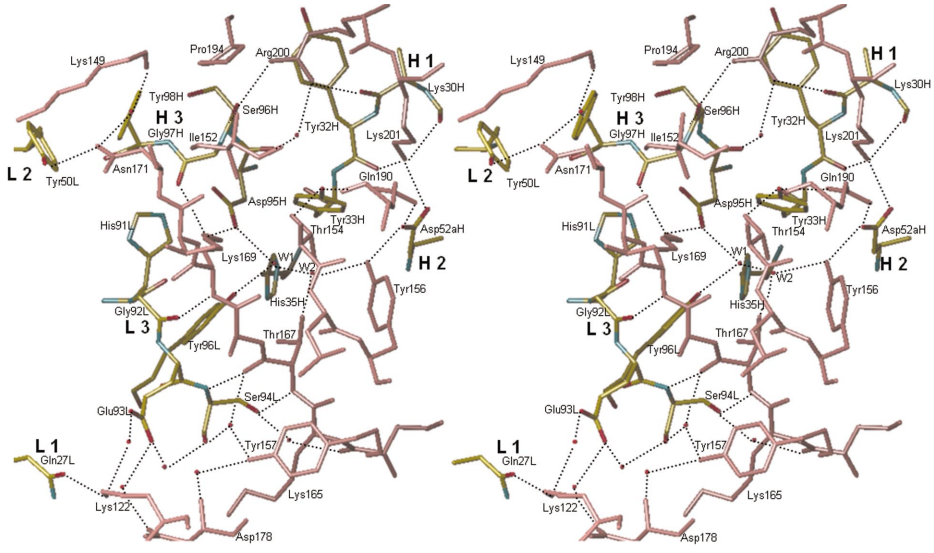

Figure 2

Stereo representation of the binding interface. The view is from TF toward the Fab. Fab and TF residues are drawn with sticks, and water molecules with spheres. TF residues are drawn in pink. Hydrogen bonds are shown in broken lines. This figure was prepared with TURBO–FRODO (Roussel & Cambillau, 1995).

3.3. Comparison with the other anti-TF antibodies

The Fab structures of anti-TF antibodies 5G9 (Huang *et al*., 1998) and D3H44 (Faelber *et al*., 2001), each in complex with TF, have been reported at the resolutions of 3.0 Å and 1.85 Å, respectively. Major differences among the 5G9, D3H44, and hATR-5 structures are observed in the H3 residues interacting with the C and C' strands of TF. The CDRs of D3H44 and hATR-5 are mutually superimposable with a root-mean-square (rms) difference of 0.64 Å for the main-chain atoms, while the H3 residues show a larger difference of 0.98 Å. This difference is ascribable to the bulkier side-chains of Asn 34L, Trp 96L, and Tyr 99H of D3H44, as respectively compared with Ser 34L, Tyr 96L, and Ala 99H of hATR-5. The hATR-5 side-chains compactly fill the space between V_H and V_L domains, and pull the H3 loop toward the TF C' strand.

Another difference is observed for water molecules located in the vicinity of the C and C' strands. In the hATR-5 complex, a pair of hydrogen-bonded waters, W1 and W2 hydrogen-bonded each other as shown in Figure 2, participate in the interactions with the C and C' strands: W1 is hydrogen-bonded to Tyr 96L, His 35H, and Asp 95H of the Fab, and W2 to Tyr 156 and Thr 167 of TF. In contrast to the hATR-5 complex, the D3H44 complex accommodates five water molecules in this location. The Asp 95H side-chain pulled by the L3 residues enables the salt-bridge formation between the Lys 169 N^{ζ} and Asp 95H $O^{\acute{e}1}$ atoms, whereas the corresponding residues in the D3H44 complex is mediated by a water molecule. The hATR-5 interacting with the C' strand in the extended conformation displaces water molecules from the combining interface, and optimizes recognition of TF.

The hATR-5 antibody has high affinity of 8.5×10^{-10} M^{-1} toward TF (Adachi *et al.*, 2001), and shows its affinity even in the presence of denaturing and reducing agents. The affinity to the denatured TF suggests that the recognition of epitopes such as the C' strand would be optimized for clinically effective inhibition of the TF-initiated blood coagulation.

Abbreviations used: CDR, complementarity-determining region of the antibody; L1, L2, L3, H1, H2, and H3 refer to the six CDRs. The letters L and H designate the light and heavy chains; Fab, antigen-binding fragment; rms, root-mean-square; TF, tissue factor, whose residues are not suffixed with the letters.

References

Adachi, H., Yabuta, N., Kudo, C., Saito, H., Esaki, K., Sato, K., Koga, T., Hattori, K., Takeya, H., & Suzuki, K. (2001). *The 18th Congress of the Int. Soc. on Thromb. Haemost.*, P1619.

Berger, M, Shankar, V, & Vafai, A. (2002). *Am. J. Med. Sci.* **324**, 14-30.

Brünger, A. T., Adams, P. D., Clore, G. M., DeLano, W. L., Gros, P., & Grosse-Kunstleve, R. W. (1998). *Acta Cryst. sect. D*, **54**, 905-921.

Butenas, S. & Mann, K. G. (2002). *Biochemistry*, **67**, 3-12.

CCP4 (1994). *Acta Cryst. sect. D*, **50**, 760-763.

Chothia, C., Lesk, A. M., Tramontano, A., Levitt, M., Smith-Gill, S. J., Air, G., Sheriff, S., Padlan, E. A., Davies, D., Tulip, W. R., Colman, P. M., Spinelli, S., Alzari, P. M., & Poljak, R. J. (1989). *Nature*, **342**, 877-883.

Davies D. R., Padlan E. A., & Sheriff S. (1990). *Annu. Rev. Biochem.* **59**, 439-73.

Faelber, K., Kirchhofer, D., Presta, L., Kelley, R. F., & Muller, Y. A. (2001). *J. Mol. Biol.* **313**, 83-97.

Huang, M., Syed, R., Stura, E. A., Stone, M. J., Stefanko, R. S., Ruf, W., Edgington, T. S., Wilson, I. A. (1998). *J. Mol. Biol.* **275**, 873-894.

Kabat, E. A., Wu, T. T., Perry, H. M., Gottesman, K. S., & Foeller, C. (1991). *Sequences of Proteins of Immunological Interest*, 5th edit., Public Health Service, National Institutes of Health, Bethesda, MD, USA.

Kirchhofer, D., Michael, T., Lipari, M. T., Moran, P., Eigenbrot, C., & Kelley, R. F. (2000). *Biochemistry*, **39**, 7380-7387.

Kraulis, P. J. (1991). *J. Appl. Crystallogr.* **24**, 946-950.

Laskowski, R. A., MacArthur, M. W., Mass, D. S., & Thornton, J. M. (1993). *J. Appl. Cryst.* **26**, 283-291.

Luzzati, V. (1952). *Acta Cryst.* **5**, 802-810.

Matthews, B. W. (1968). *J. Mol. Biol.* **33**, 491-497.

Mizutani, R., Miura, K., Nakayama, T., Shimada, I., Arata, Y., & Satow, Y. (1995). *J. Mol. Biol.* **254**, 208-222.

Moutain, A. & Adair, J. R. (1992). *Biotechnol. Gene. Eng.* **10**, 1-142.

Nicholls, A., Sharp, K. A. & Honig, B. (1991). *Proteins: Struct. Funct. Genet.* **11**, 281-296.

Rapaport, S. I. & Rao, L. V. (1995). *Thromb. Haemost*. **74**, 7-17.

Roussel, A. & Cambillau, C. (1995). *TURBO-FRODO Version 5.4*, Faculté de Médecine Nord, Marseille, France.

Venkateswarlu, D., Perera, L., Darden, T., & Pedersen, L. G. (2002). *Biophysical Journal*, **82**, 1190-1206.

Wakefield, T. W., Strieter, R. M., Prince, M. R., Downing, L. J., & Greenfield, L. J. (1997). *Cardiovasc. Surg.* **5**, 6-15.

Waxman, E., Ross, J. B., Laue, T. M., Guha, A., Thiruvikraman, S. V., Lin, T. C., Konigsberg, W. H., & Nemerson, Y. (1992). *Biochemistry*, **31**, 3998-4003.

Wilcox, J. N., Smith, K. M., Schwartz, S. M., & Gordon, D. (1989). *Proc. Natl Acad. Sci. USA*. **86**, 2839-2843.

Yokoyama, H., Mizutani, R., Satow, Y., Komatsu, Y., Ohtsuka, E., & Nikaido, O. (2000). *J. Mol. Biol.* **299**, 711-723.